Journal of Solid State Chemistry **158,** 61–67 (2001)
doi:10.1006/jssc.2000.9058, available online at http://www.idealibrary.com on IDEAL®

Crystal Structure of $BaV_{13}O_{18}$

Kouta Iwasaki,*,[1] Hirotsugu Takizawa,* Kyota Uheda,* Tadashi Endo,* and Masahiko Shimada†

*Department of Materials Chemistry, Graduate School of Engineering, Tohoku University, Aoba-yama 07, Sendai, Miyagi 980-8579, Japan; and
†Institute for Advanced Materials Processing, Tohoku University, Katahira, Sendai, Miyagi 980-8577, Japan

Received August 10, 2000; in revised form November 14, 2000; accepted December 8, 2000

Single crystals of $BaV_{13}O_{18}$ ($V^{+2.62}$) containing a small amount of Cr (about 7% of vanadium sites) were prepared by heating a mixture of $BaCO_3$, V_2O_5, V, and Cr powders at 1973 K for 40 h in flowing Ar. Crystal structure analysis using single-crystal data (Rigaku AFC7R, 4037 reflections) showed that the $BaV_{13}O_{18}$ has a rhombohedral unit cell with $a_h = 12.621(5)$ Å, $c_h = 7.020(5)$ Å, $V = 968.4(9)$ Å^3, $Z = 3$, $D_{cal} = 5.595$ g·cm^{-3}, and space group $R-3$ ($R_1 = 1.96\%$, w$R_2 = 3.60\%$, $S = 1.095$). In the structure, Ba and O formed a cubic close-packed arrangement and every V was coordinated by six O. $BaV_{13}O_{18}$ has three kinds of vanadium environments: one almost regular octahedral site and two distorted octahedral sites. VO_6 octahedra share their corners and edges. © 2001 Academic Press

Key Words: **barium vanadate; low-valence vanadium ion; single-crystal X-ray study; crystal structure analysis; V–V (cation–cation) bond; magnetic property.**

INTRODUCTION

Many vanadium complex oxides have been reported so far. However, there are few reports on complex oxides containing low-valence vanadium ions even though vanadium ions show various valence states (V^{2+}–V^{5+}). When metal ions are in low valence states in oxides, they are positioned close to each other compared to the case where metal ions are in high valence states. The metal–metal bonds in oxides, which would give anomalous crystal structures such as NbO and its homologous phases $A_nNb_{n+3m}O_{3n+3m}$ (2–10), are very interesting in terms of crystal chemistry. In addition, the electrical and magnetic properties exhibited by both metallic and ionic bonding characters are remarkable. Ti and V have larger ionic radii than other 3*d* transition metals. If they are positioned close to each other, formation of metal–metal bonds by overlapping of 3*d* orbitals is expected.

Barium vanadates containing low-valence vanadium ions have been studied in our work, and $BaV_{14}O_{19}$ (monoclinic system with $a = 7.654$ Å, $b = 12.639$ Å, $c = 7.011$ Å, $\beta = 107.8°$, and $V = 645.6$ Å^3) was reported as a new compound (1). Our studies on substitutions of Ti, Cr, and Nb for V in $BaV_{14}O_{19}$ revealed the rapid grain growth of $Ba(V,Cr)_{14}O_{19}$ by solid-state reaction, resulting in the formation of single crystals for structure determination. The preliminary crystal structure analysis made it clear that the real chemical composition of the compound was $BaV_{13}O_{18}$ ($V^{+2.62}$) and the crystal system was rhombohedral. The lattice parameters calculated using X-ray diffraction (XRD=) data were $a_h = 12.636$ Å and $c_h = 7.013$ Å. In this paper, the crystal structure of $BaV_{13}O_{18}$ determined from the single-crystal X-ray analysis is reported.

EXPERIMENTAL

Preparation of Single Crystals

Powders of $BaCO_3$, V_2O_5, V, and Cr were used as starting materials and they were mixed according to the composition $BaV_{13}CrO_{19}$. The mixture was pressed into a pellet and put into a Mo foil. A radio-frequency induction furnace was used to prepare single crystals. The sample was heated at 1973 K (the temperature was raised to this value within 1 h) for 40 h in flowing Ar and was cooled to room temperature. After the heat treatment, black elongated spherical grains ($\sim$100 μm in diameter) were obtained. The XRD pattern of the resultant sample was indexed the same as $BaV_{13}O_{18}$, and the presence of small amounts of unidentified impurities was also observed. When the XRD data for lattice parameters were recorded, Si was used as an internal standard. Figure 1 shows the lattice parameters of $BaV_{13-x}Cr_xO_{18}$. The lattice parameters of $BaV_{13-x}Cr_xO_{18}$ increase with increasing x, indicating a possible substitution of high-spin Cr^{2+} (ionic radius 0.80 Å) for V^{2+} (0.79 Å) (11). However, further studies are necessary to investigate the valence state of Cr ions in $BaV_{13-x}Cr_xO_{18}$. The lattice parameters of the resultant sample are $a_h = 12.638$ Å and $c_h = 7.022$ Å. These values are slightly smaller than those of $BaV_{12}CrO_{18}$, and the Cr content in the resultant sample is estimated to be about 7% of V sites.

[1] To whom correspondence should be addressed. Fax: +81-22-217-7228. E-mail: kouta@ain.che.tohoku.ac.jp.

0022-4596/01 $35.00

TABLE 1
Experimental Conditions and Crystallographic Parameters of $BaV_{13}O_{18}$

Temperature/K	293
Diffractometer	Rigaku AFC7R
Method	ω–2θ
2θ range	$4^\circ \le 2\theta \le 60^\circ$
Max. $\sin(\theta)/\lambda/\text{Å}^{-1}$	0.7035
Range of h, k, l	$-17 \le h \le 17$, $-17 \le k \le 17$, $-9 \le l \le 9$
Crystal shape	Elongated spherical
Crystal size/μm	50–70
Standard reflections	3 (every 150 reflections)
No. of measured reflections	4037
No. of unique reflections	635
Absorption correction	ψ scan
Chemical formula	$BaV_{13}O_{18}$
Chemical formula weight	1087.56
Space group	R-3 (No. 148)
Cell formula units Z	3
a_h/Å	12.621(5)
c_h/Å	7.020(5)
V/Å^3	968.4(9)
$D_{cal}/g \cdot cm^{-3}$	5.595
$\mu(MoK\alpha)/cm^{-1}$, λ/Å	12.03, 0.71069
T_{max}/T_{min}	0.548/0.458
RR/RR'	1.064/1.038
R_{int}	0.0496
R_σ	0.0291
R_1 ($F_o > 4\sigma(F_o)$)/R_1 (all)	0.0166/0.0196
wR_2	0.0360
Goodness of fit	1.095
$(\Delta/\sigma)_{max}$	0.001
$\Delta\rho_{max}/\Delta\rho_{min}$/e Å^{-3}	0.499/−0.648

Crystal Structure Determination

X-ray diffraction data of the single crystals were collected by using a Rigaku AFC-7R X-ray diffractometer using monochromatized Mo$K\alpha$ radiation. The details of data collection conditions are summarized in Table 1. All reflections were recorded during the data collection.

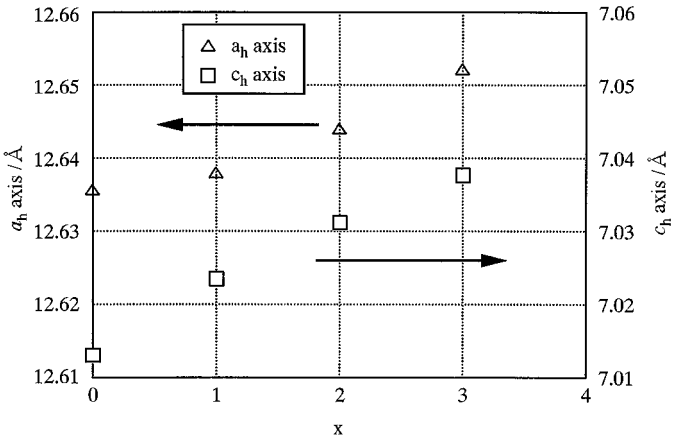

FIG. 1. The lattice parameters of $BaV_{13-x}Cr_xO_{18}$.

Sir97 (12) was used to solve the crystal structure and Shelxl (SHELX97-2) (13) was used for crystal structure refinement. All observed reflections (4037 reflections) were used in the structure refinement. Space groups R-3 (No. 148) and $R3$ (No. 146, acentric) were possible, and both space groups led to the same crystal structures in the present study. As a result, R-3 was adopted because its symmetric property was higher than that of $R3$. Incidentally, the absolute structure was not determined in $R3$; Flack's parameter χ was not close to 0 or 1. The Cr content in the single crystal was small (about 7% of vanadium sites) and the atomic scattering of Cr was comparable to that of V, so that the amount of chromium and its position were not refined. Because $BaV_{13}O_{18}$ seemed to be stoichiometric as mentioned below, the occupancy in each crystallographic site

TABLE 2
Atomic Coordinates and Temperature Factors of $BaV_{13}O_{18}$

Atom	Site	x	y	z	U_{eq}	
Ba	3a	0.0000	0.0000	0.0000	0.00690(9)	
V(1)	3b	0.0000	0.0000	0.5000	0.0085(2)	
V(2)	18f	0.05050(3)	0.43636(3)	0.50393(5)	0.00691(9)	
V(3)	18f	0.49112(3)	0.93163(3)	0.17608(5)	0.00829(10)	
O(1)	18f	0.47507(12)	0.79055(12)	0.0036(2)	0.0080(3)	
O(2)	18f	0.17079(12)	0.40933(13)	0.6587(2)	0.0076(3)	
O(3)	18f	0.03574(12)	0.29019(12)	0.3419(2)	0.0071(3)	
Atom	U_{11}	U_{22}	U_{33}	U_{23}	U_{13}	U_{12}
Ba	0.00661(10)	0.00661(10)	0.00748(13)	0.000	0.000	0.00331(5)
V(1)	0.0106(2)	0.0106(2)	0.0044(3)	0.000	0.000	0.00528(11)
V(2)	0.0050(2)	0.0059(2)	0.0094(2)	−0.00162(11)	−0.00159(10)	0.00240(11)
V(3)	0.0075(2)	0.0094(2)	0.0091(2)	0.00315(11)	0.00108(11)	0.00511(13)
O(1)	0.0070(6)	0.0065(6)	0.0104(7)	0.0007(4)	0.0005(5)	0.0034(5)
O(2)	0.0063(6)	0.0109(7)	0.0065(7)	−0.0004(5)	−0.0011(5)	0.0050(5)
O(3)	0.0065(6)	0.0077(6)	0.0076(7)	0.0009(4)	0.0011(4)	0.0040(5)

TABLE 3
X-Ray Powder Diffraction Data of $BaV_{13}O_{18}$ Indexed as Hexagonal *R*-3, $a_h = 12.621$ Å, $c_h = 7.020$ Å

h	*k*	*l*	d_{obs}/Å	d_{calc}/Å	I/I_0	*h*	*k*	*l*	d_{obs}/Å	d_{calc}/Å	I/I_0
1	1	0	6.304	6.3095	1	−3	−4	1	1.7424	1.7404	2
						4	3	1			
3	0	0	3.651	3.6428	8						
						1	0	4	1.7310	1.7311	2
−1	−2	1	3.566	3.5591	30						
2	1	1				0	2	4	1.6698	1.6694	4
						−1	−4	3			
0	1	2	3.343	3.3388	19	−4	−1	3			
						1	4	3			
2	2	0	3.161	3.1548	23	4	1	3			
2	0	2	2.954	2.9511	9	−6	−1	1	1.6228	1.6214	1
						1	6	1			
1	3	1	2.7864	2.7823	16						
−3	−1	1				−4	−3	2	1.6003	1.5990	4
						3	4	2			
−2	−1	2	2.6752	2.6732	6						
1	2	2				7	0	1	1.5256	1.5239	3
						−5	−3	1			
4	0	1	2.5497	2.5457	8	3	5	1			
4	1	0	2.3885	2.3848	10	−3	−1	4	1.5180	1.5176	2
1	4	0				1	3	4			
−2	−3	1	2.3640	2.3608	6	−1	−6	2	1.5067	1.5052	3
3	2	1				6	1	2			
0	0	3	2.3373	2.3377	3	−2	−6	1	1.4832	1.4813	2
						6	2	1			
−1	−3	2	2.2956	2.2931	7						
3	1	2				7	1	0	1.4493	1.4475	17
						1	7	0			
−1	−1	3	2.1925	2.1921	14						
1	1	3				−2	−3	4	1.4373	1.4368	23
						3	2	4			
3	3	0	2.1064	2.1032	4	0	6	3			
						6	0	3			
0	5	1	2.0902	2.0867	1						
						0	7	2	1.4277	1.4262	2
−3	−2	2	2.0414	2.0395	100	−3	−5	2			
2	3	2				5	3	2			
−4	−2	1	1.9840	1.9812	5	−2	−5	3	1.4021	1.4009	3
2	4	1				−5	−2	3		1.4009	
0	3	3	1.9686	1.9674	2	2	5	3			
3	0	3				5	2	3			
−1	−5	1	1.8926	1.8902	4	0	1	5	1.3929	1.3912	1
5	1	1				−6	−2	2			
						2	6	2			
5	0	2	1.8569	1.8549	4						
						3	6	0	1.3787	1.3769	2
−2	−4	2	1.7814	1.7795	2	6	3	0			
4	2	2									
						−4	−5	1	1.3737	1.3722	2
5	2	0	1.7524	1.7499	3	5	4	1			
2	5	0									

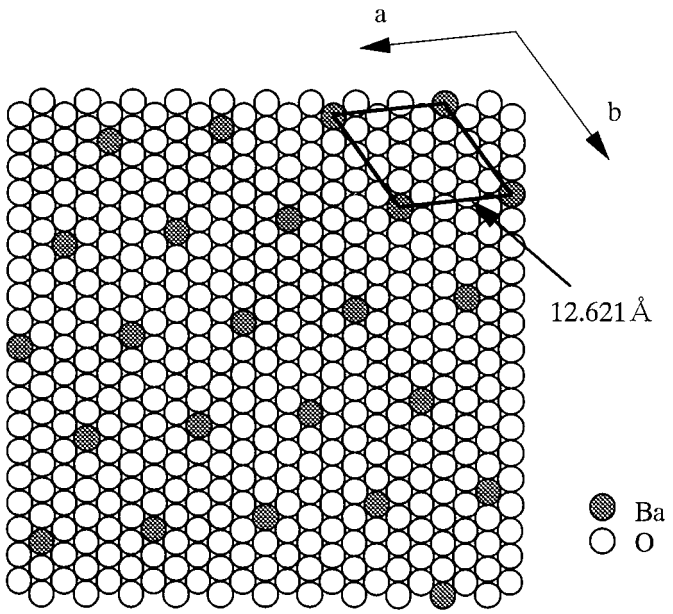

FIG. 2. The close-packed Ba–O layer in $BaV_{13}O_{18}$.

was fixed to 1. The crystallographic parameters are also listed in Table 1, and atomic coordinates and temperature factors of $BaV_{13}O_{18}$ are given in Table 2.

RESULTS AND DISCUSSION

XRD Data

The XRD data of $BaV_{13}O_{18}$ are given in Table 3. The d_{calc} is the value calculated from the single-crystal data. $BaV_{13}O_{18}$ can be synthesized by heat treatments in the temperature range 1573–2273 K in flowing Ar. Varying the heating temperature, the heating time, and the starting composition did not cause significant peak shifts in the XRD pattern of $BaV_{13}O_{18}$, indicating that $BaV_{13}O_{18}$ is stoichiometric.

Description of Crystal Structure

Barium and oxygen ions form a cubic close-packed arrangement. Figure 2 shows the close-packed Ba–O layer. The layer is stacked along the *c* axis with one-third shift in the direction of [− 1,1,0] as shown in Fig. 3. $BaV_{13}O_{18}$ has three kinds of vanadium sites positioned in the interstices of oxygen ions (see Fig. 4), and every vanadium is coordinated by six oxygen ions to form a VO_6 octahedron. The arrangement of VO_6 octahedra is also shown in Fig. 4 ($BaV_{13}O_{18}$ does not have a layer structure although the figure is depicted like a layer structure). VO_6 octahedra link by sharing their corners and edges. Such linkages of VO_6 octahedra and formation of a Ba–O close-packed arrangement are commonly found in Ba–V–O compounds containing

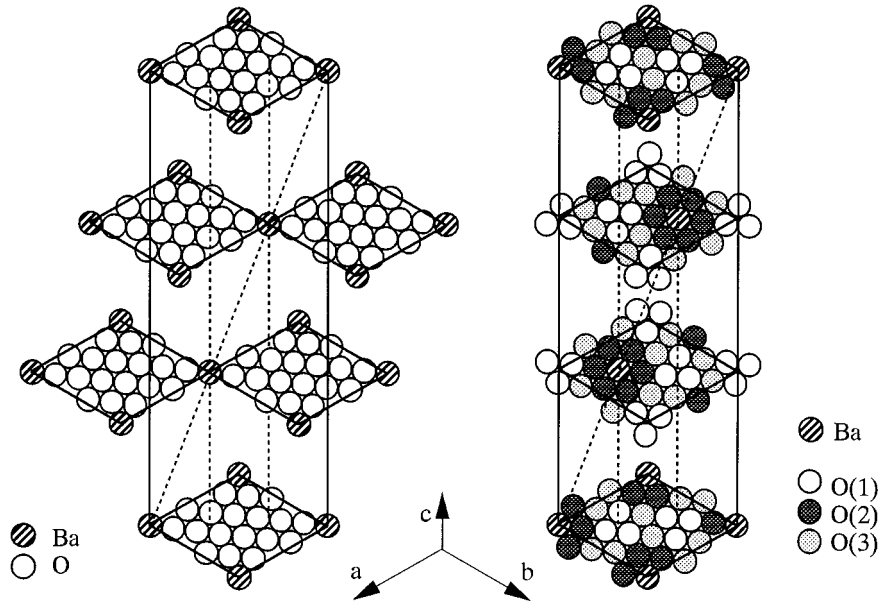

FIG. 3. The stacking of close-packed layers and positions of O sites in $BaV_{13}O_{18}$.

low-valence vanadium ions, $BaV_{10}O_{15}$ ($V^{+2.8}$) (14) and $BaV_{10-x}O_{17}$ ($V^{+3.2-3.4}$) (15).

Interatomic distances are given in Table 4. Barium is coordinated by six O(2) atoms in the same *c* plane (see Fig. 3) and six O(1) atoms out of the plane to form a BaO_{12} cuboctahedron. V(1) is coordinated by six O(1) atoms to form a $V(1)O_6$ octahedron. The $V(1)O_6$ octahedron is sandwiched between two BaO_{12} cuboctahedra in the direction of the *c* axis and surrounded by six $V(3)O_6$ octahedra by sharing their edges in the vertical direction of the *c* axis. V(3) is located around V(1) across shared octahedral edges in the same *c* plane as shown in Fig. 4 and coordinated by two O(1), one O(2), and three O(3) atoms to form a $V(3)O_6$ octahedron. V(2) is coordinated by one O(1), three O(2), and two O(3) atoms to form a $V(2)O_6$ octahedron. V(2) and V(3) are surrounded by eight and nine vanadium ions, respectively, across shared octahedral edges.

Figure 5 shows the $V(1)O_6$, $V(2)O_6$, and $V(3)O_6$ octahedra. The $V(1)O_6$ octahedron is nearly regular. On the other hand, the $V(2)O_6$ octahedron has the most distorted form of all. The average V–O distance in the $V(3)O_6$ octahedron is the longest among the three kinds of VO_6 octahedra. The average V–O distances are 2.039 Å, 2.032 Å, and 2.048 Å in $V(1)O_6$, $V(2)O_6$, and $V(3)O_6$, respectively.

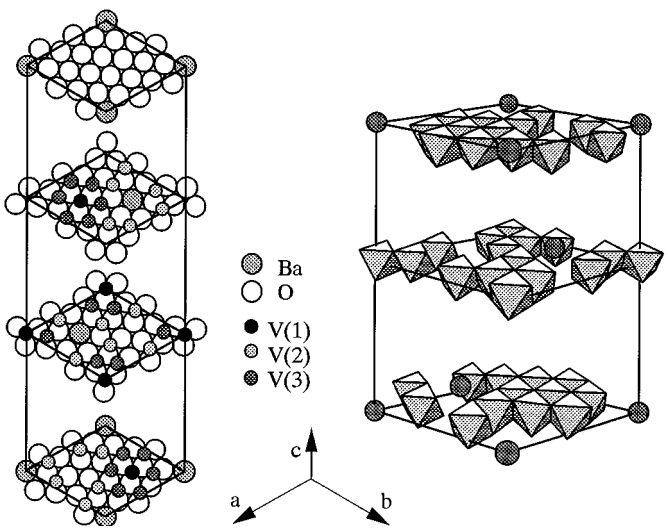

FIG. 4. The positions of V sites and the arrangement of VO_6 octahedra.

TABLE 4
Interatomic Distances (Å) in $BaV_{13}O_{18}$

Ba–O(1) × 6	2.905(2)				
Ba–O(2) × 6	2.846(2)				
V(1)–O(1) × 6	2.039(2)				
V(1)–V(3) × 6	2.9143(12)				
V(2)–O(1)	2.019(2)				
V(2)–O(2)	1.979(2)	1.991(2)	2.030(2)		
V(2)–O(3)	2.078(2)	2.095(2)			
V(2)–V(2)	2.5012(12)	3.0464(14)	3.0464(14)		
V(2)–V(3)	2.7162(14)	2.723(2)	3.049(2)	3.055(2)	3.073(2)
V(3)–O(1)	1.989(2)	2.078(2)			
V(3)–O(2)	2.036(2)				
V(3)–O(3)	2.071(2)	2.030(2)	2.085(2)		
V(3)–V(1)	2.9143(12)				
V(3)–V(2)	2.7162(14)	2.723(2)	3.049(2)	3.055(2)	3.073(2)
V(3)–V(3)	2.9166(12)	2.9166(12)	2.959(2)		

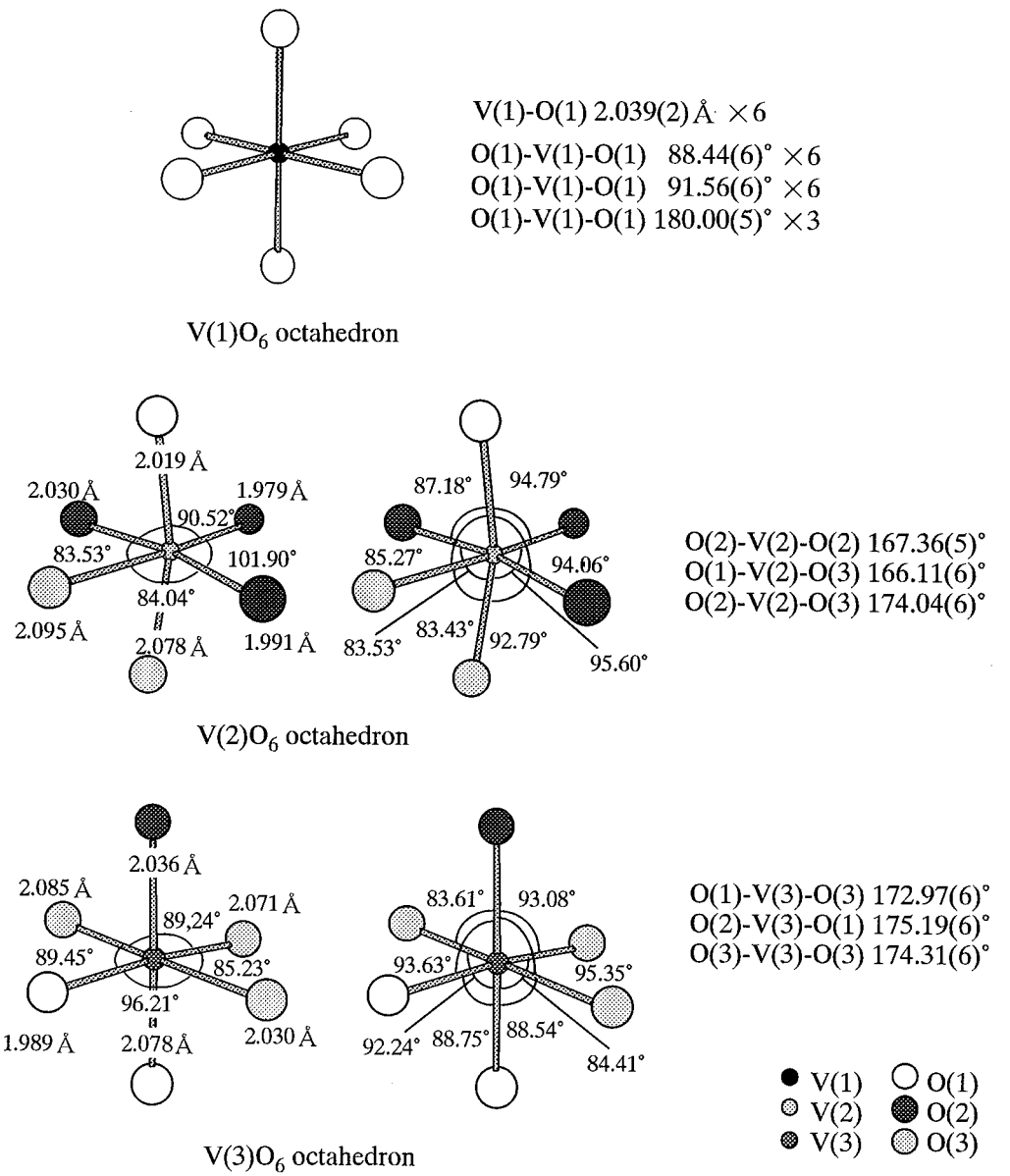

FIG. 5. Diagrams of VO_6 octahedra.

Distribution of V Ions

Assuming that $BaV_{13}O_{18}$ contains only V^{2+} and V^{3+}, we can describe $BaV_{13}O_{18}$ as $BaV_5^{2+}V_8^{3+}O_{18}$. This assumption seems to be probable because each vanadium site has the same coordination number. The bond-valence sum for $BaV_{13}O_{18}$ was calculated with the valence state of vanadium ion being +3, and the result is given in Table 5. The value at the V(2) site is larger than those of the V(1) and V(3) sites. The largest value of bond-valence sum and the shortest average V–O distance would indicate that the V(2) site is mostly occupied by V^{3+} (ionic radius 0.64 Å) (11). In the same way, V^{2+} (0.79 Å) would occupy the V(3) site

TABLE 5
Bond-Valence Calculations for $BaV_{13}O_{18}$[a]

Ba	2.474
V(1)	2.694
V(2)	2.765
V(3)	2.641
O(1)	2.031
O(2)	2.177
O(3)	2.059

[a] Calculated with the valence state of V being +3.

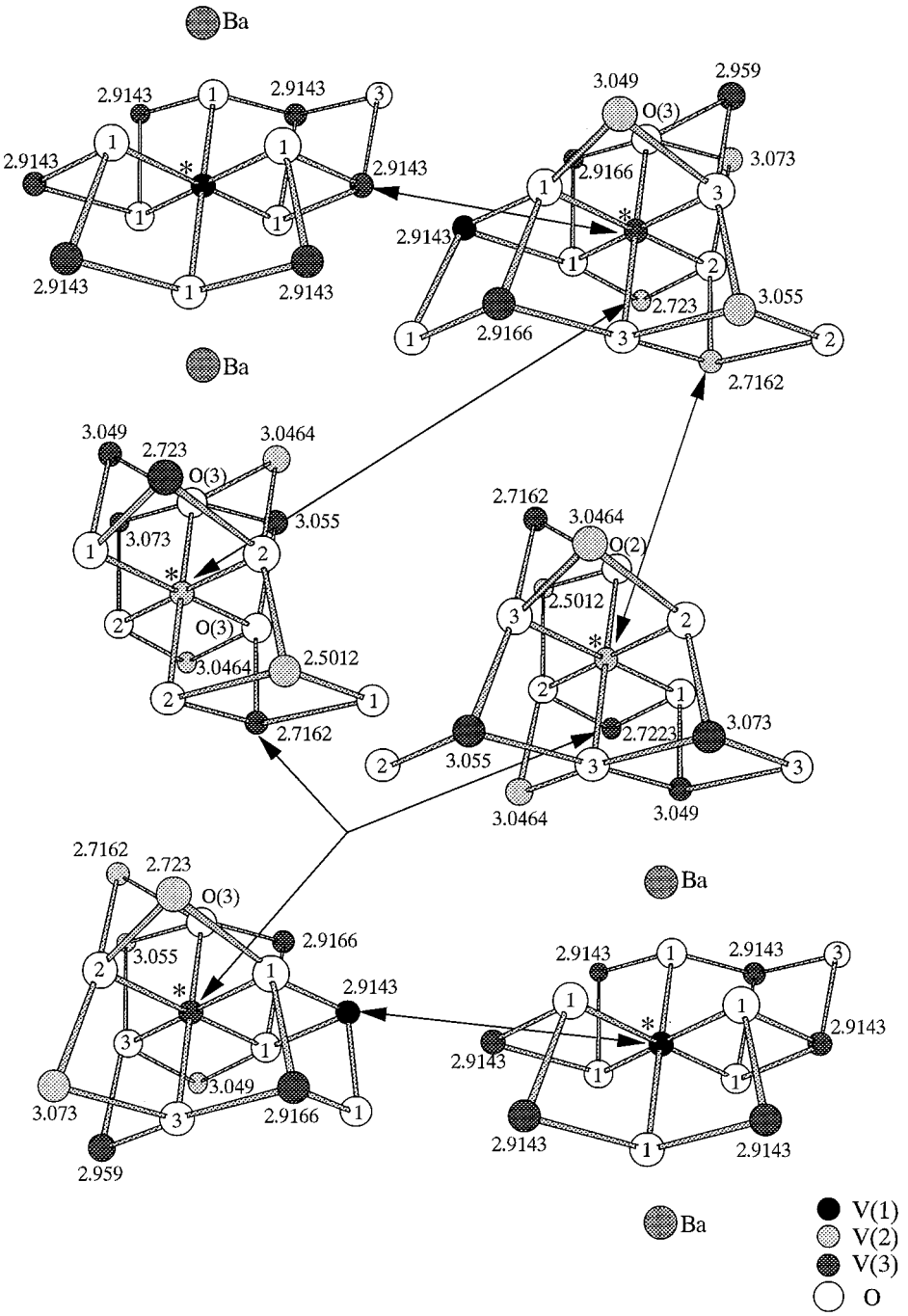

FIG. 6. The diagram of V(1)–V(3)–V(2)–V(3)–V(1) configuration. The asterisk shows the centric V in the VO_6 octahedron. The number in a white circle shows the O site given in Table 2. The value near the V shows the distance (Å) from the centric V (see Table 4).

preferably because it has the smallest value of bond-valence sum and the longest average V–O distance. However, it should be pointed out that the $V(1)O_6$ octahedron (the average V–O distance of 2.039 Å) is nearly the same as the regular VO_6 octahedron in rock-salt-type VO (V–O distance of 2.04 Å (16, 17)) and the $V(1)O_6$ octahedron is considered to be capable of being occupied by V^{2+}.

As mentioned above, the crystal contains a small amount of Cr ions (about 7% of vanadium sites), and Cr ion seems to be high-spin Cr^{2+}. The ionic radius of high-spin Cr^{2+} (0.80 Å) is larger than that of V^{2+} (0.79 Å), so Cr^{2+} is also considered to occupy V(1) or V(3) sites, like V^{2+}. In addition, Cr^{2+} would occupy a V(3) site, to take into account that high-spin Cr^{2+} (d^4) displays the Jahn–Teller effect. The

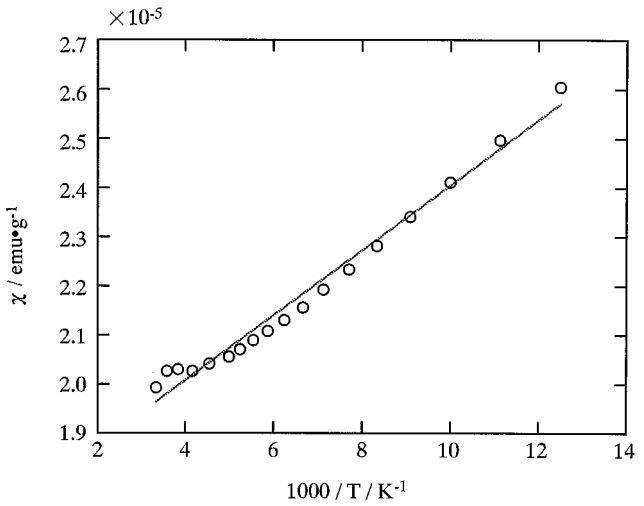

FIG. 7. Temperature dependence of magnetic susceptibility of $BaV_{13}O_{18}$.

$V(1)O_6$ octahedron is nearly regular and not appropriate for high-spin Cr^{2+} (d^4) compared to the $V(3)O_6$ octahedron containing different V–O distances.

It may not be possible to determine the charge distribution of vanadium and chromium ions because of the formation of cation–cation bonds throughout the structure as discussed below. The cation–cation bonds are considered to result in a mixed itinerant and localized character of vanadium ions.

V–V (Cation–Cation) Bonds

The critical V–V distance for cation–cation bond formation is reported to be 2.94 Å (18). V–V distances in $BaV_{13}O_{18}$ are from 2.5012 to 3.073 Å as given in Table 4. Attending to V–V distances of 2.94 Å or less, we can confirm the continuous V–V link throughout the structure; for example, V(1)–V(3)–V(2)–V(3)–V(1) as shown in Fig. 6. From a structural point of view, the possibility of V–V bond formation is suggested.

The measurement of the temperature dependence of magnetic susceptibility was carried out by using single-phase $BaV_{13}O_{18}$, and the result is shown in Fig. 7. $BaV_{13}O_{18}$ exhibited paramagnetic behavior with an effective Bohr magneton number of 0.073. The small value of the effective Bohr magneton number is due to the delocalization of 3*d* electrons, indicating the formation of V–V bonds. When every 3*d* electron delocalizes, $BaV_{13}O_{18}$ should exhibit Pauli paramagnetism. The slight localization of 3*d* electrons in $BaV_{13}O_{18}$ would result from the localized level caused by the 3*d* orbital which does not form a V–V bond because of the out-of-critical distance for the cation–cation bond.

The metallic character of delocalized 3*d* electrons and electron hoppings of localized 3*d* electrons are expected to have an effect on the electrical conductivity of $BaV_{13}O_{18}$. Electrical conductivity measurement of $BaV_{13}O_{18}$ revealed the semiconductor behavior with an electrical conductivity of the order of 10^2 $S \cdot cm^{-1}$ in the temperature range of 80–300 K.

SUMMARY

In this study, the crystal structure of $BaV_{13}O_{18}$ was determined by single-crystal X-ray study. The crystal structure and magnetic behavior suggested the possible formation of V–V bonds in $BaV_{13}O_{18}$. Low-valence-state metal ions would cause the reduction of an ionic bond, destabilizing compounds. However, when cation–cation bonds are formed, they are expected to stabilize the structure. Although there have been few reports on compounds containing low-valence-state metal ions before now, new compounds will be found.

ACKNOWLEDGMENTS

K.I. thanks Dr. Yamane (Institute for Advanced Materials Processing, Tohoku University) for his help with the crystal structure analysis.

REFERENCES

1. K. Iwasaki, H. Takizawa, K. Uheda, T. Endo, and M. Shimada, *Trans. Mater. Res. Soc. Jpn.* **25,** 1163 (2000).
2. G. Svensson, *J. Solid State Chem.* **90,** 249 (1991).
3. G. Svensson, J. Köhler, and A. Simon, *J. Alloys Compd.* **176,** 123 (1991).
4. G. Svensson, J. Köhler, and A. Simon, *Angew. Chem., Int. Ed. Engl.* **31,** 212 (1992).
5. C. E. Michelson, P. E. Rauch, and F. J. DiSalvo, *Mater. Res. Bull.* **25,** 971 (1990).
6. G. Svensson, *Acta Chem. Scand.* **44,** 222 (1990).
7. G. Svensson, J. Köhler, and A. Simon, *Acta Chem. Scand.* **46,** 244 (1992).
8. G. Svensson, *Mater. Res. Bull.* **23,** 437 (1988).
9. V. G. Zubkov, A. P. Tyutyunnik, V. A. Pereliaev, G. P. Shveikin, J. Köhler, R. K. Kremer, A. Simon, and G. Svensson, *J. Alloys Compd.* **226,** 24 (1995).
10. G. Svensson and L. Eriksson, *J. Solid State Chem.* **114,** 301 (1995).
11. R. D. Shannon, *Acta Crystallogr. A* **32,** 751 (1976).
12. A. Altomare, M. C. Burla, M. Camalli, G. L. Cascarano, C. Giacovazzo, A. Guagliardi, A. G. G. Moliterni, G. Polidori, and R. Spagna, *J. Appl. Crystallogr.* (*Denmark*) **32,** 115 (1999).
13. G. M. Sheldrick, "SHELX97," University of Göttingen, Germany, 1997.
14. D. C. de Beaulieu and H. Müller-Buschbaum, *Z. Naturforsch. Teil B, Anorg. Chem., Org. Chem.* **35,** 669 (1980).
15. Y. Kanke, E. Takayama-Muromachi, K. Kato, and K. Kosuda, *J. Solid State Chem.* **113,** 125 (1994).
16. S. Westman and C. Nordmark, *Acta Chem. Scand.* **14,** 465 (1960).
17. S. Takeuchi and K. Suzuki, *J. Jpn. Inst. Metals* **31,** 611 (1967). [in Japanese]
18. J. B. Goodenough, "Progress in Solid State Chemistry," Vol. 5, Chap. 4, Pergamon, New York, 1971.